

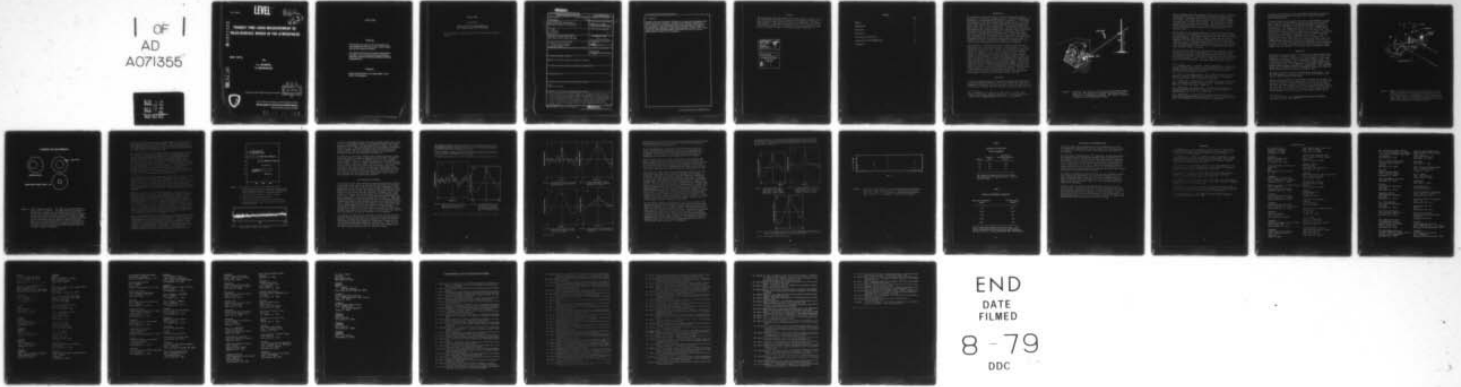
AD-A071 355

ARMY ELECTRONICS RESEARCH AND DEVELOPMENT COMMAND WS--ETC F/G 4/2
TRANSIT TIME LIDAR MEASUREMENT OF NEAR-SURFACE WINDS IN THE ATM--ETC(U)
MAY 79 T L BARBER, R RODRIGUEZ
ERADCOM/ASL-TR-0033

UNCLASSIFIED

NL

| OF |
AD
A071355



END
DATE
FILMED
8-79
DDC

ASL-TR-0033

LEVEL *II*

AD
Reports Control Symbol
OSD - 1366

12
BS

AD A 071 355

TRANSIT TIME LIDAR MEASUREMENT OF NEAR-SURFACE WINDS IN THE ATMOSPHERE

MAY 1979

By

**T.L. BARBER
R. RODRIGUEZ**

DDC FILE COPY

DDC
RECEIVED
JUL 19 1979
REGULATED
D

Approved for public release; distribution unlimited



US Army Electronics Research and Development Command
Atmospheric Sciences Laboratory
White Sands Missile Range, NM 88002

79 07 18 003

NOTICES

Disclaimers

The findings in this report are not to be construed as an official Department of the Army position, unless so designated by other authorized documents.

The citation of trade names and names of manufacturers in this report is not to be construed as official Government indorsement or approval of commercial products or services referenced herein.

Disposition

Destroy this report when it is no longer needed. Do not return it to the originator.

ERRATA SHEET

ASL-TR-0033

TRANSIT TIME LIDAR MEASUREMENTS OF
NEAR SURFACE WINDS IN THE ATMOSPHERE

Reverse graphs for figures 6B and 7B. Figure captions remain as they are.

UNCLASSIFIED

10 ERADCOM/ASL-TR-4733

SECURITY CLASSIFICATION OF THIS PAGE (When Data Entered)

REPORT DOCUMENTATION PAGE		READ INSTRUCTIONS BEFORE COMPLETING FORM
1. REPORT NUMBER ASL-TR-0033	2. GOVT ACCESSION NO.	3. RECIPIENT'S CATALOG NUMBER 9 Research and development
4. TITLE (and Subtitle) TRANSIT TIME LIDAR MEASUREMENT OF NEAR-SURFACE WINDS IN THE ATMOSPHERE		5. TYPE OF REPORT & PERIOD COVERED R&D Technical Report
7. AUTHOR(s) T. L. Barber R. Rodriguez		6. PERFORMING ORG. REPORT NUMBER
9. PERFORMING ORGANIZATION NAME AND ADDRESS Atmospheric Sciences Laboratory White Sands Missile Range, NM 88002		8. CONTRACT OR GRANT NUMBER(s) 17/14
11. CONTROLLING OFFICE NAME AND ADDRESS US Army Electronics Research and Development Command Adelphi, MD 20783		10. PROGRAM ELEMENT, PROJECT, TASK AREA & WORK UNIT NUMBERS 16 DA Task No. 1L161102B53A14
14. MONITORING AGENCY NAME & ADDRESS (if different from Controlling Office)		12. REPORT DATE 11 May 1979
		13. NUMBER OF PAGES 30 (12) 35p
		15. SECURITY CLASS. (of this report) UNCLASSIFIED
		15a. DECLASSIFICATION/DOWNGRADING SCHEDULE
16. DISTRIBUTION STATEMENT (of this Report) Approved for public release; distribution unlimited.		
17. DISTRIBUTION STATEMENT (of the abstract entered in Block 20, if different from Report)		
18. SUPPLEMENTARY NOTES		
19. KEY WORDS (Continue on reverse side if necessary and identify by block number) Lidar Remote wind sensing		
20. ABSTRACT (Continue on reverse side if necessary and identify by block number) This report deals with an improved model of a transit time laser radar. The technique measures a backscatter signal from atmospheric aerosols from two sample volumes a known distance apart in the atmosphere. These two signals are cross-correlated to obtain the time of flight of aerosol inhomogeneities as they move from one volume to another. Once the time of flight is calculated, the windspeed can be obtained since the distance between sample volumes is known. This model utilizes a copper vapor laser as the transmitter source. (Cont'd)		

DD FORM 1 JAN 73 1473 EDITION OF 1 NOV 65 IS OBSOLETE

UNCLASSIFIED

SECURITY CLASSIFICATION OF THIS PAGE (When Data Entered)

410 663

JOB

20. (Cont'd)

Crosswind data were successfully obtained in the unperturbed atmosphere under very clear, and thus difficult, conditions with horizontal visibility of 130 km. Results of the experiments showed that even under these conditions the variability of the aerosol concentration was high enough to permit a correlation that generated a reliable wind measurement at least once a minute. Transit time lidar wind measurements agreed within 15 percent of values simultaneously recorded with an anemometer.

PREFACE

The authors thank Mr. Noah Montoya of the Meteorological Support Division for his skillful assistance in calibrating and manning the range gate system during the data collection phase of the experiment. The authors also thank Dr. H. Auvermann from the Physical Science Laboratory at New Mexico State University for the skillful computer programming and mathematical techniques he used in reducing the complex lidar data.

Accession For	
NTIS GRA&I	<input checked="" type="checkbox"/>
DDC TAB	<input type="checkbox"/>
Unannounced	<input type="checkbox"/>
Justification	<input type="checkbox"/>
By _____	
Distribution/	
Availability Codes	
Dist	Avail and/or special
A	

CONTENTS

	Page
PREFACE	1
INTRODUCTION	3
BACKGROUND	3
METHODOLOGY	6
DATA ANALYSIS AND RESULTS	11
CONCLUSIONS AND RECOMMENDATIONS	18
REFERENCES	19

INTRODUCTION

The atmospheric wind field affects the United States Army Tactical operations. For example, the impact point of a ballistic projectile is affected by crosswinds prevailing along its trajectory. If the gunner has knowledge of the wind structure before aiming the gun, he can make the necessary corrections to achieve improved and more accurate fire-power. This will, in turn, increase the first-round-hit probability and standoff range of our friendly forces. Optical remote wind sensors have displayed the potential capability of providing the wind structure information along the forward trajectory of ballistic projectiles. This report discusses the experimental setup of a prototype transit time lidar system (TTL), an optical remote wind sensor, and presents some preliminary data collected with the system. TTL is an exploratory development prototype of an active remote crosswind sensor that is capable of measuring crosswind speed (component perpendicular to the laser beam) at predetermined small volumes in the atmosphere.

The TTL method of measuring wind velocity depends on the fact that atmospheric dust is not uniformly mixed in the atmosphere. As these inhomogeneities or particulate patterns are carried by the wind, they change as a function of time. However, during the sample period of the TTL, the change is so small it is assumed to be nil. The TTL transmits a pulsed laser beam which illuminates two predetermined volumes in the atmosphere. The distance between these two sample volumes is determined by the geometry of the receiving telescope (optical receiver) shown in figure 1. A set of photomultipliers converts the backscattered light energy into two electrical signals. To determine range, the electrical signals are gated by the ranging circuit in the electronic receiver. These two gated signals are then digitized and cross-correlated to extract the transit time, which is the time needed by the pattern to travel from one volume to the other. With this transit time and distance between sample volumes, the perpendicular wind component (magnitude and direction) can be calculated.

BACKGROUND

In the past, three methods to measure winds remotely with lidar have received considerable attention. These three methods are based on the phenomenon that aerosols in the atmosphere move with the same velocity as the wind. Schwiesow¹ has used the doppler principle with a CO₂ lidar

¹R. L. Schwiesow, R. E. Cupp, M. J. Post, and R. F. Calfee, 1977, "Coherent Differential Doppler Measurements of Transverse Velocity at a Remote Point," Applied Optics, Vol 16, No. 5, pp 1145-1150

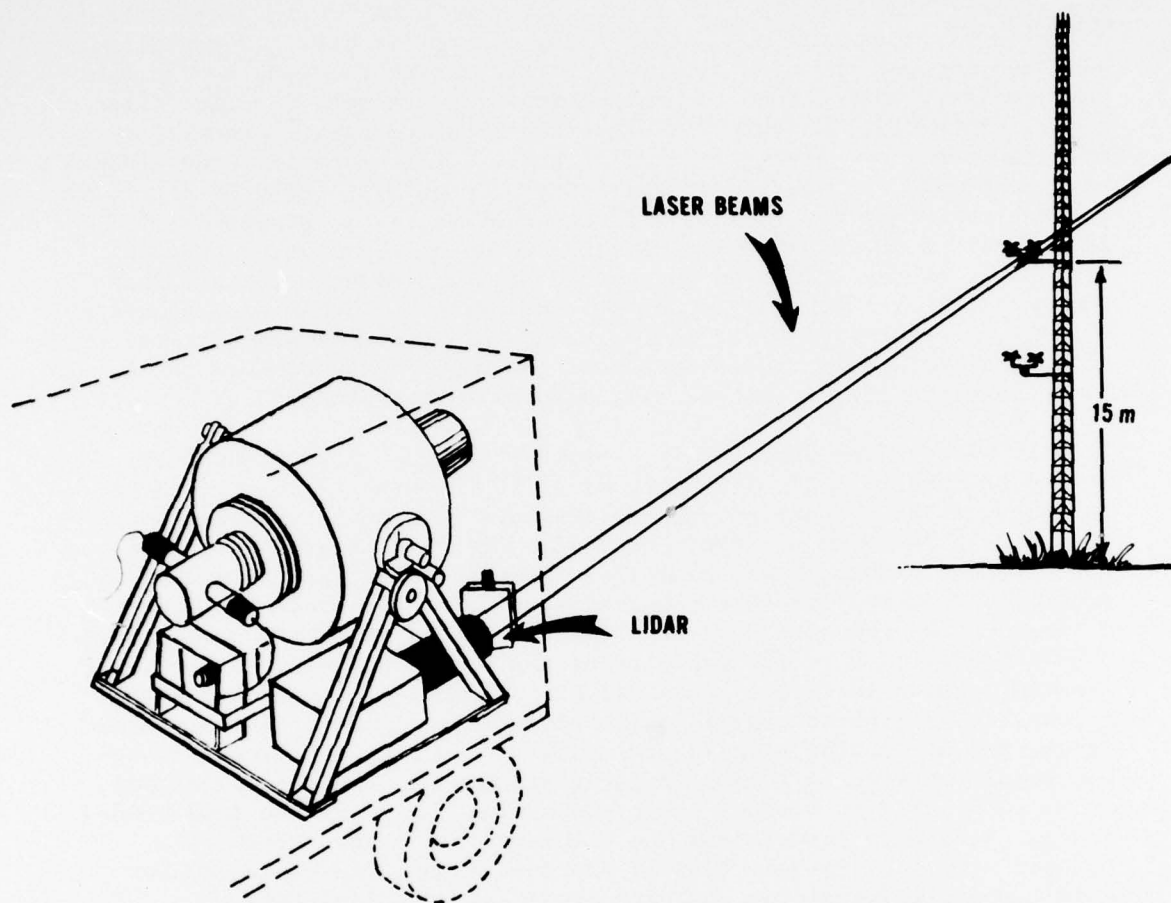


Figure 1. A sketch of the lidar field setup at LC 36, White Sands Missile Range, NM. The transmitter is a copper vapor laser, and the receiver is a cassegrainian telescope. The reference anemometer is attached to the meteorological tower.

system to measure the radial component of the wind velocity. Leuthner² has measured the motion of large dust conglomerates (approximately 1,000 m wide) to determine wind velocity in two dimensions at ranges up to 10 km. This second method requires at least 2.5 min to obtain sufficient data to compute wind velocity. The third method is known as the transit time lidar (TTL) approach. Derr³ has done some preliminary work in this area; however, Barber and Mason⁴ have conducted most of the advanced work in this area, including development of a prototype model.

The TTL effort at this laboratory began in 1972 when a nitrogen laser was utilized as the transmitter and an electronic range gate was used in the receiver.^{4,5} This approach proved that the TTL method of remotely measuring windspeed was feasible. However, there were two obvious drawbacks: (1) the pulse repetition frequency (prf) of the nitrogen laser was very slow, forcing the sample volumes to be too far apart to obtain meaningful correlations; (2) the beam divergence of the nitrogen laser was approximately 6 mrad, which did not permit efficient use of laser energy at ranges of interest.

To alleviate these problems, the nitrogen laser was replaced with an argon ion laser in 1974. During this phase of the experiment, energy per pulse was determined to be insufficient; furthermore, the laser was extremely sensitive to vibration and therefore could not be employed in field experiments.⁶ Thus, in 1977 a copper vapor laser was substituted as the TTL transmitter. The copper vapor laser with a beam

²T. G. Leuthner and E. W. Eloranta, "Remote Measurements of Longitudinal and Crosspath Wind Velocities with a Monostatic Lidar," paper presented at the 8th International Laser Radar Conference at Drexel University, Philadelphia, PA, June 1977

³V. F. Derr, G. M. Lerfald, and M. J. Post, 1978, "Measures of Inhomogeneity of Aerosols," ERADCOM Report ASL-CR-78-8017-1. Atmospheric Sciences Laboratory, White Sands Missile Range, NM

⁴T. L. Barber and J. B. Mason, 1974, "A Transit-Time Lidar Wind Measurement: A Feasibility Study," ECOM Report 5550. Atmospheric Sciences Laboratory, White Sands Missile Range, NM

⁵R. L. Armstrong, J. B. Mason, and T. L. Barber, 1976, "Detection of Atmospheric Aerosol Flow Using a Transit-Time Lidar Velocimeter," Applied Optics, Vol 15, No. 11, pp 2891-2995

⁶T. L. Barber and R. B. Loveland, "The Transit-Time Laser Radar as a Remote Wind Measuring Device," paper presented at the 7th International Laser Radar Conference at SRI Menlo Park, CA, November 1975

divergence of less than 0.5 mrad concentrated more energy per pulse in a given volume of atmosphere, had much better stability, and had a sufficiently high prf.

The laser energy from the copper vapor laser is approximately 1 mJ per pulse, which is the same amount of energy available from the nitrogen laser. However, because of its large beam divergence, only about 0.1 percent of the radiation from the nitrogen laser illuminated the sample volumes. The copper vapor laser has a beam collimator which concentrates all the available energy in a 2-cm circle at 70 m. (The beam collimator and the method of producing the two beams are illustrated in figure 2.) In addition, ultraviolet light is scattered more efficiently than visible light by atmospheric particulates.⁷ These two factors increase the scatter return per pulse by a factor of 37. Furthermore, the pulse repetition rate increased 100 times (from 60 to 6,000), thereby increasing the potential information rate by a factor of 3,700. The copper vapor laser was more adaptable to field operations because it is not very susceptible to mechanical vibrations or thermal changes, and also because it is relatively easily and quickly aligned.

METHODOLOGY

The method of measuring winds by illuminating two sample volumes with a single laser is shown in figure 2. As the laser beam comes out of the collimator, it strikes a director front surface mirror. After being reflected, the beam goes to the two staggered pointing mirrors. Each of these mirrors intercepts half of the circular beam and reflects it to the sample volume. The illumination of each sample volume is maximized by adjusting each pointing mirror independently. The transmitted energy that is backscattered by the atmospheric particles is collected by the optical receiver, a telescope focused at 70 m.

The copper vapor laser outputs two wavelengths simultaneously: 5106 and 5782 angstroms. About three-fourths of the total energy is produced at the 5106-angstrom wavelength.

Figure 3 shows a diagram of the alignment procedure that was used. As the laser is turned on, the copper starts to heat up and a fluorescent output is visible on a sheet of paper placed in front of the laser. The first dim output produced is blue with a slow transition to pink, then to green. If the optics have not been aligned previously, the output might look like figure 3A. The first step is to adjust the rear mirror micrometer until an output like that shown in figure 3B is

⁷H. C. Van de Hulst, 1957, Light Scattering by Small Particles, John Wiley and Sons, Inc., New York

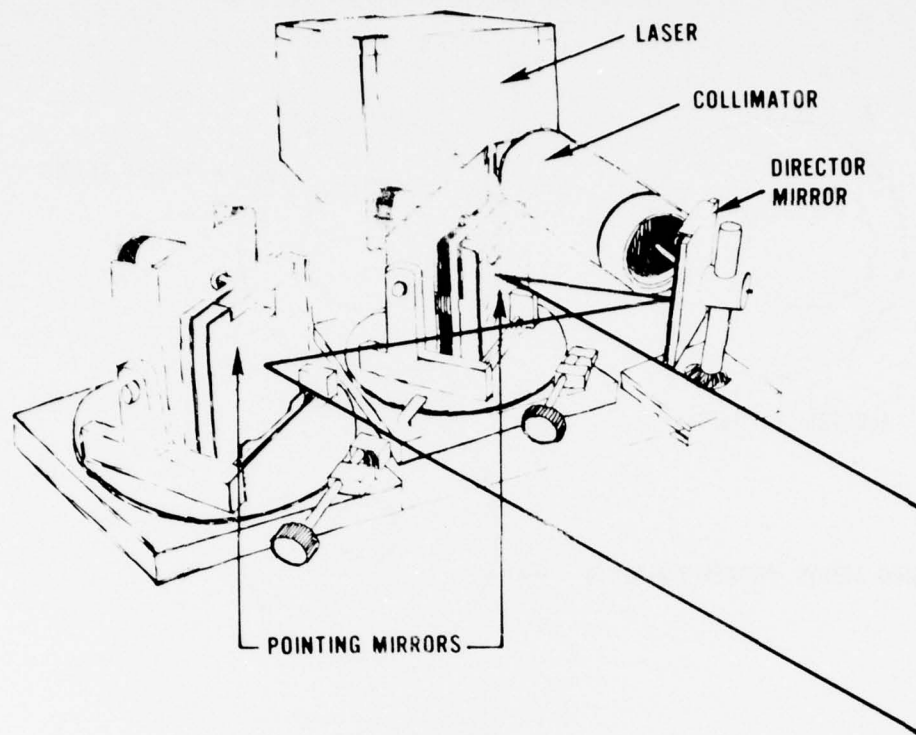


Figure 2. Method of forming two beams from a single laser. The main beam is expanded by the collimator and then redirected by the director mirror. The pointing mirrors are staggered in such a manner that each intercepts and reflects half of the beam. These mirrors can be adjusted individually to obtain efficient illumination of the sample volumes.

LASER ALIGNMENT

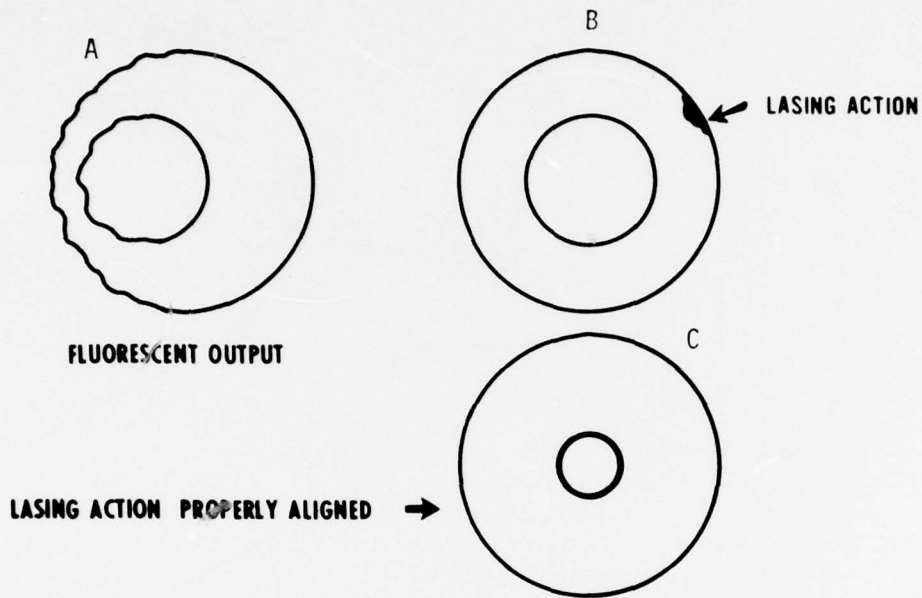


Figure 3. Laser alignment procedure. "A" shows the condition when the laser is out of alignment. The image produced by the laser on a white piece of paper is a dim green image with the inner portion only slightly brighter than the outer portion. Adjusting the rear reflector produces condition "B" where the image is still dim green, but the inner portion is centered. At this point, lasing action will be visible as shown by the arrow. Next, a no. 14 welder goggle plate is placed in the beam, and the front reflector is adjusted to achieve the condition at "C" where the inner section is relatively brilliant green and the edge is evenly illuminated.

obtained. At this point a welder's goggle number 14 is placed at the laser output port to reduce the intensity. The second step is to adjust the front mirror micrometer to go from 3B to the shape shown in 3C. When the optics are properly aligned, the laser spot becomes circular and its edge is brilliant and even.

The scattered light from the sample volumes collected by the telescope is converted to an electrical signal by a pair of photomultipliers. Both of these wavelengths are transmitted into the atmosphere, but a 20-angstrom optical filter in front of the photomultiplier tubes, centered at 5106 angstroms, reduces the extraneous light noise and passes the major frequency of the laser. The signal from each of the two photomultipliers is fed to a gate circuit. A time sequence of this gate circuit operation is presented in figure 4. The signal that is obtained through the gate circuit from one photomultiplier is an average return from an atmospheric volume of 4 m in length and 2 cm in diameter at a range of 70 m. The other photomultiplier gated signal is from a similar volume horizontally displaced 24 cm.

The data from each gate are recorded on an analog tape recorder together with the three analog signals from a UVW/anemometer. One of the anemometer's sensors is lined up perpendicular to the laser beam as shown in figure 1. A synchronizing pulse (data flag) is also recorded. The data from these tapes are digitized by using the synchronizing pulse as reference, waiting 50 microseconds, and reading a voltage value from photomultiplier 1, photomultiplier 2, and the perpendicular wind component.

Figure 5 is a sample of the backscatter return. The exact source of the high frequency variations in the backscattered signal is unknown. However, results from previous experimentation and theoretical considerations have shown that the data of interest will fall in the frequency range of 0.1 to 30 Hz. This is corroborated by considering an average windspeed of 10 m/sec and dust irregularities from 0.5 m to 10 m diameter. In the case of the dust irregularity having a size of 0.5 m and moving at 10 m/sec, it will take 0.05 sec for the irregularity to go through the beam, which is equivalent to a frequency of 20 Hz. In the case of a 10-m diameter dust irregularity going through the beam, when the wind blows at 10 m/sec, the transit time will be 1 sec, which is equivalent to a frequency of 1 Hz.

The total information recorded on analog tape is dependent on the laser pulse repetition rate which is a key characteristic in determining the maximum wind velocities which can be ascertained. Information theory states that at least three pulses are needed per atmospheric volume illuminated as a particulate pattern travels through the two probed volumes. As mentioned before, in the case of the nitrogen laser, TTL operation was limited because its maximum prf was only 100 Hz. To minimize these problems and to insure collection of proper data as

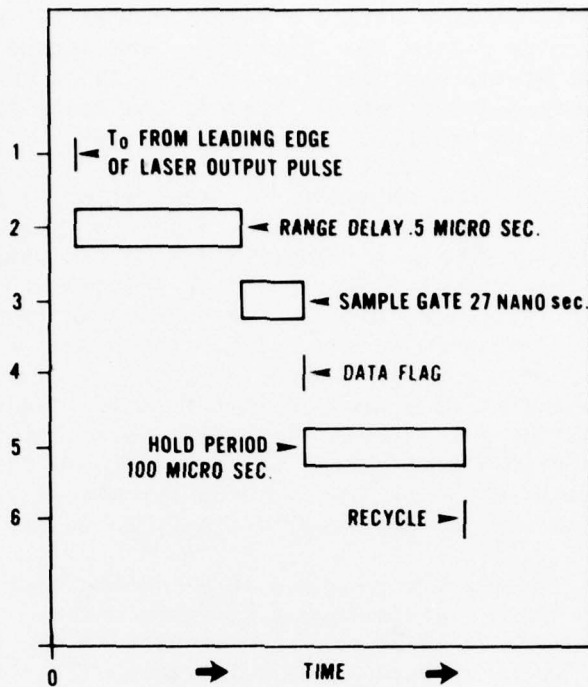


Figure 4. Time sequence of gate circuit operation (one cycle).

- 1 - electronic pulse produced by a photodiode looking at the surface reflection from one of the laser cavity windows. This is the sync pulse that starts gate operation.
- 2 - range delay from transmitter to sample volume.
- 3 - sample volume length determination.
- 4 - data flag to initiate sampling by the A/D converter.
- 5 - period during which signal is held until A/D converter finishes sampling.

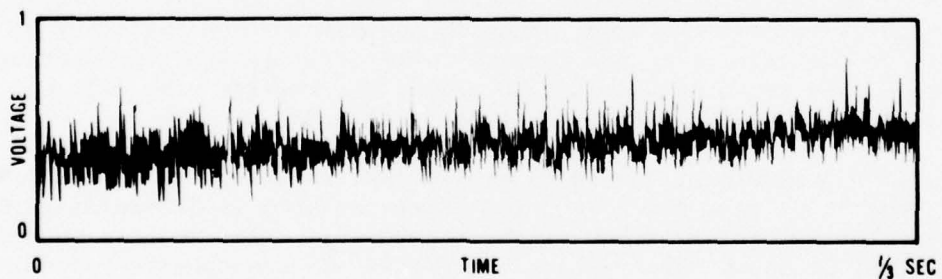


Figure 5. Plot of gated backscattered voltage signal vs time. Note the high frequency content in the signal.

required by information theory, the distance between samples was chosen as 1.2 m. With these constraints, the maximum windspeed that could be measured was 16.6 m/sec. For low winds, such as 1 m/sec, the transit time was 1.2 sec. During this time period, the atmospheric particulate pattern changed appreciably; therefore, there was less correlation between signals. As the correlation decreased, the probability of obtaining a reliable wind measurement decreased too.

The problem was resolved by replacing the nitrogen laser with a copper vapor laser which is capable of generating prf from 800 to 10,000 Hz. It was decided to use a prf of 6,000 Hz, and 24 cm as the distance between samples. With this improved configuration, a low wind velocity, such as 1 m/sec, produces a transit time of 0.24 sec. If the operating prf is 6,000 Hz, then 1,440 pulses occur during the transit time. Furthermore, the transit time is so short that deterioration of the atmospheric particulate patterns is negligible. When high winds, such as 50 m/sec are present, the transit time becomes 1/208 sec; in this time interval, the copper vapor laser generates 29 pulses, which is quite adequate for the computational algorithm.

DATA ANALYSIS AND RESULTS

As illustrated in the last paragraph of the preceding section, the frequency ranges which contain the desired wind information are inversely proportional to the size of the existent turbulent atmospheric cells. Knowing that at the 15-m altitude probed the dust irregularities, which backscatter the lidar signal, are carried in turbulent cells of a size range 5 to 20 m and that the wind velocities of interest fall in the vicinity of 10 m/sec, the TTL data should lie in the frequency range below 30 Hz. However, the raw data collected contained many high frequency components, as shown in the sample plot of figure 5. These high frequency variations in the data had the effect of producing "unclear" correlations, which in turn generated unrealistically high wind velocity values. Figures 6A through 6F show examples of such correlations; the most striking examples are the correlograms of figures 6B and 6C which yielded the extremely high velocity values of 240 and 180 m/sec, respectively. Sources of the high frequency components include "pulse-to-pulse" variations in the laser output, microstructures in the particulate concentration, and optical turbulence in the atmosphere.

To eliminate the high frequency components from the raw data and thus decrease the error in the results, a computer filtering subroutine was employed. The algorithm used by this subroutine consists of Fourier-transforming the raw data, removing all undesirable frequencies, and then inverse Fourier-transforming the resultant data. Since the data are removed or filtered by a computer, the high cutoff frequency and the type of filter roll-off curve can readily be changed.

The data shown in this series of figures were Fourier-transformed and passed through a filter with a cosine squared high frequency roll-off and a 3 dB point at 45 Hz. Figures 6A through 6F were produced with consecutive data blocks, covering a total time period of 4.2 sec. The point in time at which these data were taken is shown in figures 8 and 9 by an arrow.

These six correlations are presented to illustrate problems produced by the high frequency components (4 to 45 Hz) in the data. These high frequencies can be related to the shape effect of the dust cells and optical turbulence in the atmosphere along the laser beam.

The average wind velocity measured by the reference anemometer during this time period was 4.75 m/sec.

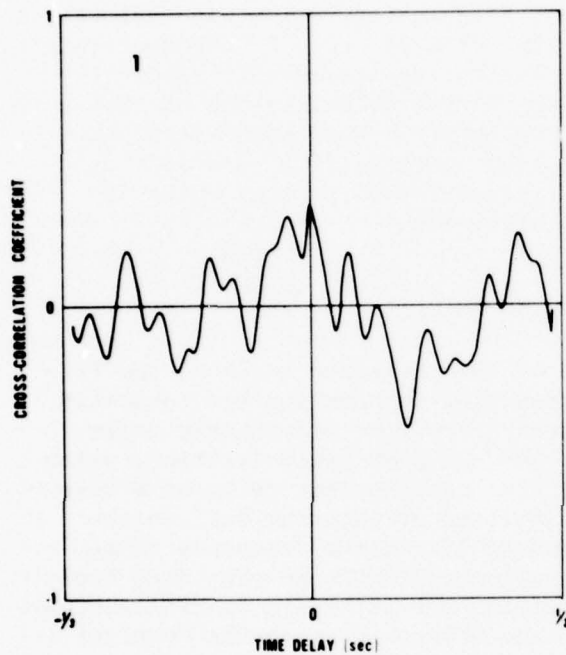


Figure 6A. Cross-correlation with a poorly defined maxima. Three peaks with a similar maximum amplitude are present. Calculated wind velocity 22.3 m/sec.

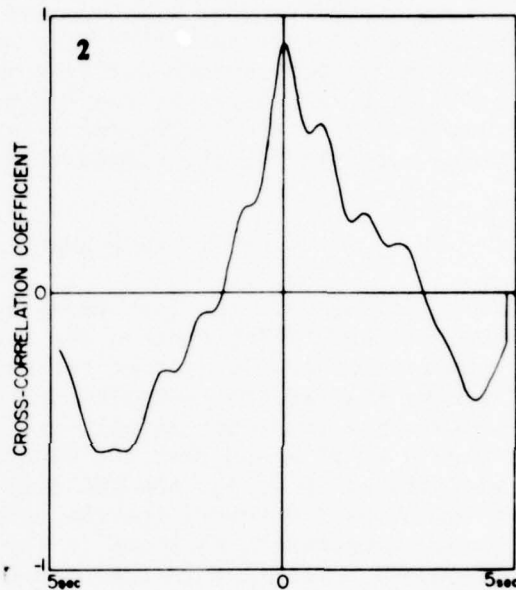


Figure 6B. A well-defined cross-correlation but unrealistically high calculated wind velocity of 180 m/sec. Time delay between graph ordinate and correlation maximum is 0.0013 sec.

Figure 6. Cross-correlation of two data blocks, each with 4096 data points taken at a rate of 6000 Hz.

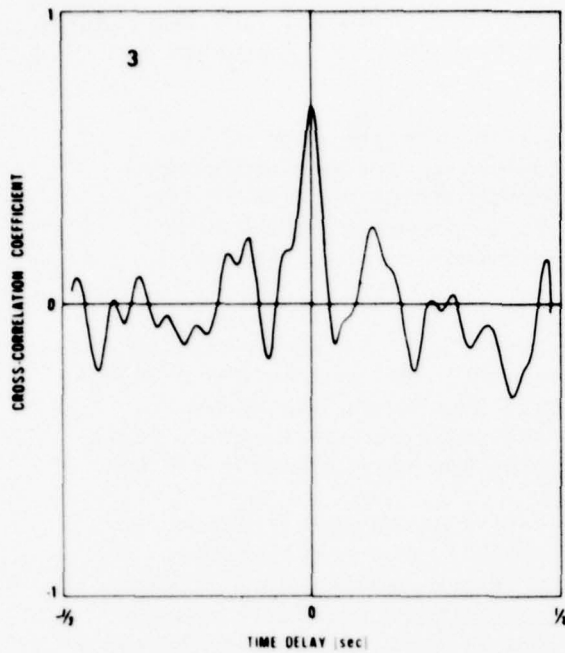


Figure 6C. A well-defined cross-correlation maximum, but unrealistically high calculated wind velocity: 240 m/sec.

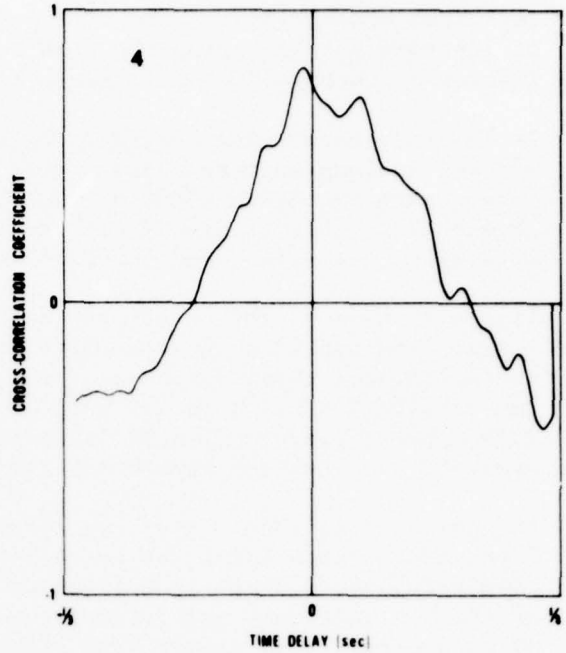


Figure 6D. Cross-correlation with a single, but somewhat broad, maximum. Calculated wind velocity: 31.3 m/sec.

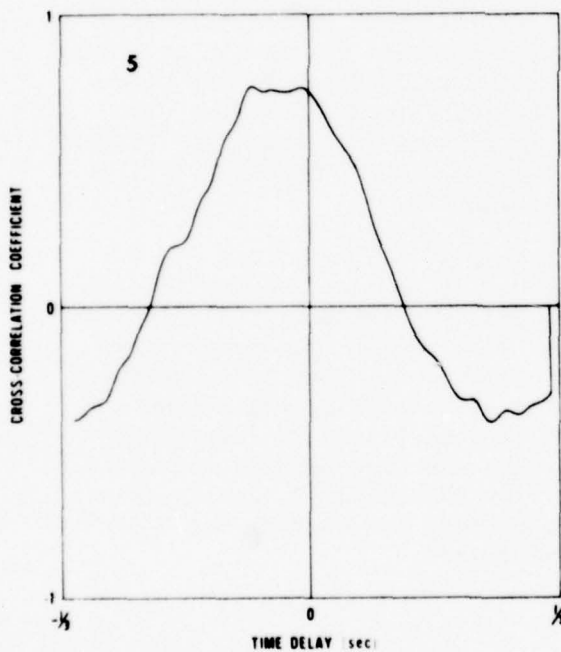


Figure 6E. Cross-correlation with a poorly defined broad correlation maximum. Calculated wind velocity: 9.1 m/sec.

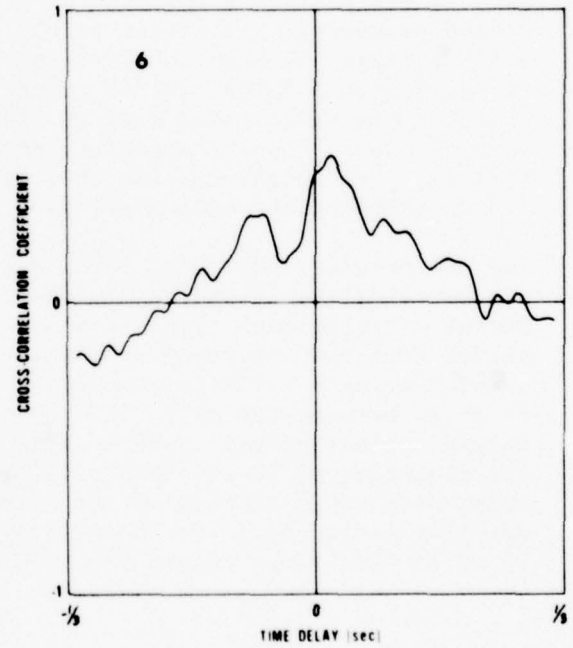


Figure 6F. Cross-correlation with a broad and poorly defined maximum. Calculated wind velocity: 3.3 m/sec.

Figure 6. (cont)

Empirical evaluations of the filtered data were conducted, and the results of incrementally changing the high cutoff frequency are presented in figures 7A through 7C and in table 1.

As the most meaningful correlations occurred when the size of the aerosol inhomogeneities ranged from 1 to 8 m, it became important to investigate how often these aerosol inhomogeneities show up in the atmosphere. This frequency of occurrence is important because it determines how often wind velocity measurements can be obtained.

Figure 8 shows a plot of the sum of the first ten low frequency harmonics, and experiments determined that when this sum exceeded 0.25 of the highest total value, a cross-correlation which provided meaningful results for the data collected in this experiment was obtained. This type of pattern of dust inhomogeneity was found to occur at least every 60 sec when the horizontal visibility was approximately 130 km.

Two parameters, sample time and filter band-pass characteristics, were found to be quite important in obtaining meaningful correlations. A meaningful correlation is defined as one that generates a comparison of the TTL wind data and reference anemometer data within 15 percent of each other. The sample time affected the shape of the correlogram's maximum, which in turn produced "unclear" correlations. Sample times of 0.67, 2.0, 4.67, and 10.0 sec were evaluated, and the conclusion was that the 4.67 sec sample time produced correlograms with a single, well-defined maximum and a correlation coefficient of 0.85 or greater. The second parameter of interest is the filter band-pass characteristics, which include the high cutoff frequency, low cutoff frequency, and type of roll-off. A filter with a cosine squared roll-off curve was used, and the 3 dB cutoff frequency was set at 3.0, 2.0, and 1.0 Hz. The results due to these changes are shown in figures 7A through 7C. After analysis, the conclusion was that setting the high frequency cutoff at 2.0 Hz produced the most meaningful correlograms.

The low cutoff frequencies tried were 0.2, 0.4, 0.5, 0.6, and 0.7 Hz; and empirically, it was determined that 0.6 Hz produced the most meaningful correlograms. Table 2 shows a comparison between wind velocity values from the reference anemometer and TTL. These values were computed from data collected over a 5-min period. Although fair agreement is shown between the pairs of values, the conclusion is that these values are not closer to each other because the lidar and anemometer are measuring different sample volumes, and also because the reference anemometer has a certain amount of inertia. Nonetheless, during this sampling period only one lidar wind measurement was outside the 5 to 13 m/sec wind range recorded by the anemometers.

For this series of figures, the large sample time is accomplished by obtaining a new data block of 4096 data points where each new data point is the summation of 15 old data points. The new data block was Fourier-transformed, filtered, and inverse Fourier-transformed before the cross-correlation was computed. This group of three correlograms shows the effect of varying the high cutoff frequency. Table 1 shows these same results in numerical form.

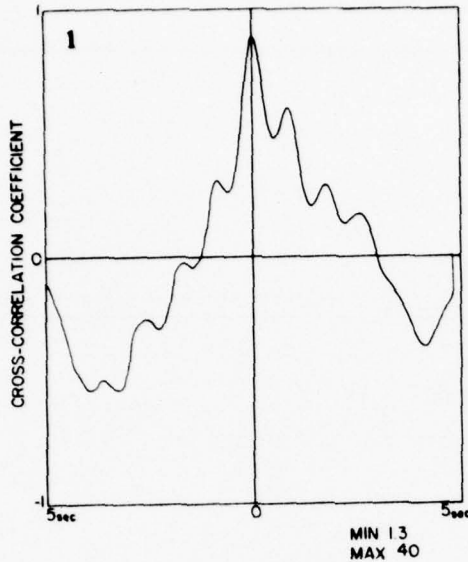


Figure 7A. A cross-correlation with a well-defined maximum. High frequency filter cutoff: 3 Hz. Calculated wind velocity: 8 m/sec. Measured wind velocity: 4.75 m/sec, 68% high.

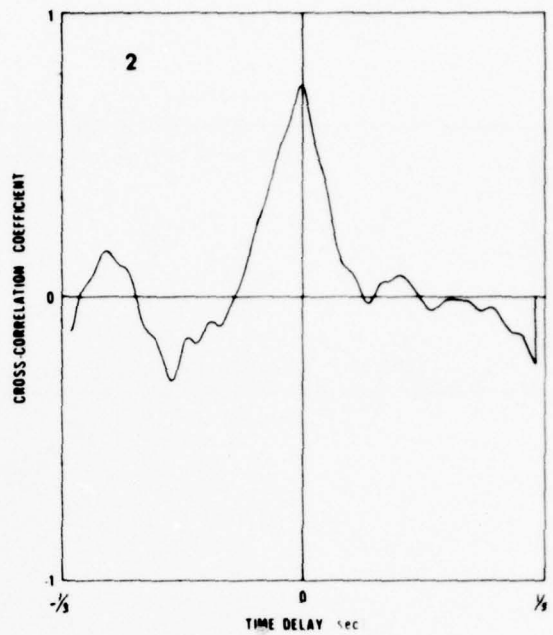


Figure 7B. A cross-correlation with a well-defined maximum. High frequency cutoff: 2 Hz. Calculated wind velocity: 5.3 m/sec. Measured wind velocity: 4.75 m/sec, 12% high. A reasonable comparison.

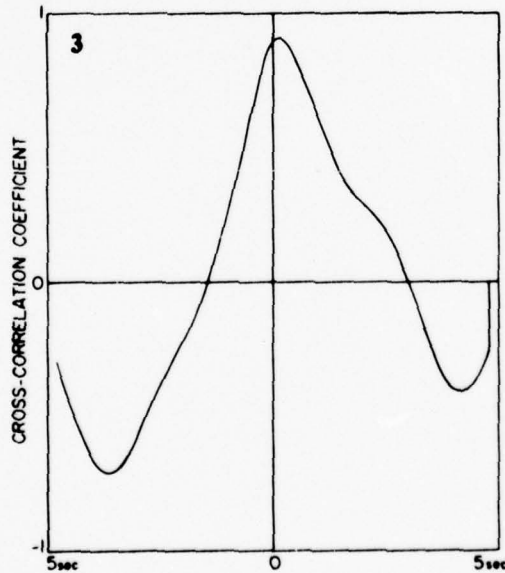


Figure 7C. A cross-correlation with a well-defined yet slightly broadened maximum. High frequency filter cutoff: 1 Hz. Calculated wind velocity: 1.2 m/sec. Measured wind velocity: 4.75 m/sec, 75% low. The frequencies from 1 to 2 Hz should not have been removed.

Figure 7. Cross-correlation of two 10-sec data blocks.

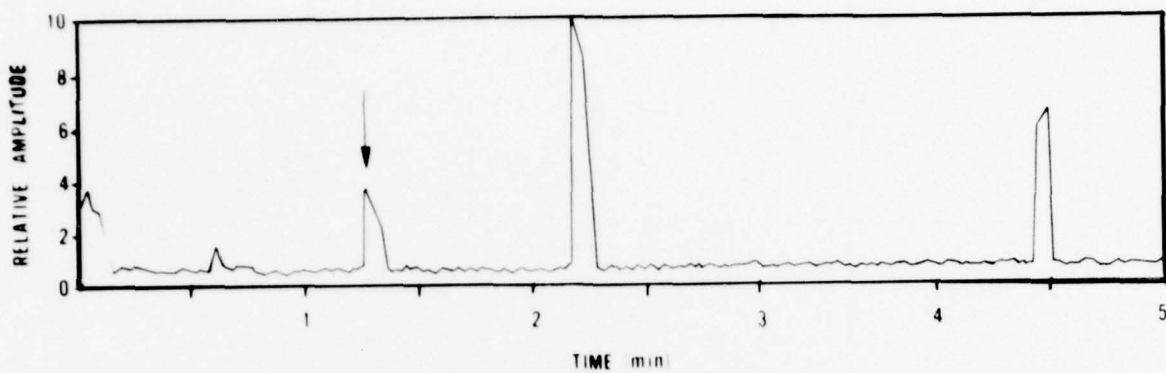


Figure 8. Time plot of the first 10 low frequency harmonics in the Fourier-transform of 4096 point data blocks. These frequencies extend from 1.5 to 15 Hz. It was empirically determined that when the curve exceeded 1.5, a meaningful correlation was obtained.

TABLE 1

SETTING OF FILTER HIGH
CUTOFF FREQUENCY

Figure	Frequency (Hz)	Calculated Crosswind Velocity (m/sec)
7A	2.9	8.0
7B	2.0	5.3
7C	1.0	1.2

The measured averaged wind velocity, during the period when the above data were collected, was 4.75 m/sec.

TABLE 2

CROSSWIND MEASUREMENT COMPARISON

Reference Anemometer (m/sec)	TTL Measurement (m/sec)
9.6	14.7
10.0	10.3
6.8	4.7
10.8	6.0
10.4	6.0

Each of these data samples was 4.67 sec long. Low cutoff frequency was 0.6 Hz and high cutoff frequency was set at 4.0 Hz. Cross-correlations were well-defined.

CONCLUSIONS AND RECOMMENDATIONS

The copper vapor laser performed well as the transmitter for the TTL. Its operational characteristics make it suitable for experimental field use because it is relatively easy to align and is not very sensitive to vibration.

With the present configuration of TTL, reasonable crosswind measurements were obtained from the unperturbed atmosphere when the visibility was approximately 130 km. The best results were obtained when a band-pass filter with a high cutoff frequency of 4 Hz and a low cutoff frequency of 0.6 Hz was used to filter the raw data from both photomultipliers. Using a sample time of 5 sec, TTL is capable of measuring crosswind at least once every 60 sec at a height of 15 m. As the horizontal visibility decreases, crosswind data can be obtained much more easily because the amount of backscatter signal increases.

The degree of agreement between TTL and the reference anemometer values can be improved by optimization of the system's parameters, such as sample volume dimensions, laser prf, and distance between sample volumes. Furthermore, this optimization will also increase the range of operation to the point where a range of 4 km in the unperturbed atmosphere seems reasonable.

The first step in a follow-up program should be analysis of all the available data. After that, data under different meteorological conditions should be obtained and reduced. A collective analysis of all the data should be sufficient to evaluate the TTL's performance. Future efforts should also include an investigation of the optimization of the mathematical algorithm. As part of this investigation, the sample time and band-pass filter characteristics should be studied.

REFERENCES

1. Schwiesow, R. L., R. E. Cupp, M. J. Post, and R. F. Calfee, 1977, "Coherent Differential Doppler Measurements of Transverse Velocity at a Remote Point," Applied Optics, Vol 16, No. 5, pp 1145-1150.
2. Leuthner, T. G., and E. W. Eloranta, "Remote Measurements of Longitudinal and Crosspath Wind Velocities with a Monostatic Lidar," paper presented at the 8th International Laser Radar Conference at Drexel University, Philadelphia, PA, June 1977.
3. Derr, V. F., G. M. Lerfald, and M. J. Post, 1978, "Measures of Inhomogeneity of Aerosols," ERADCOM Report ASL-CR-78-8017-1, Atmospheric Sciences Laboratory, White Sands Missile Range, NM.
4. Barber, T. L., and J. B. Mason, 1974, "A Transit-Time Lidar Wind Measurement: A Feasibility Study," ECOM Report 5550, Atmospheric Sciences Laboratory, White Sands Missile Range, NM.
5. Armstrong, R. L., J. B. Mason, and T. L. Barber, 1976, "Detection of Atmospheric Aerosol Flow Using a Transit-Time Lidar Velocimeter," Applied Optics, Vol 15, No. 11, pp 2891-2995.
6. Barber, T. L., and R. B. Loveland, "The Transit-Time Laser Radar as a Remote Wind Measuring Device," paper presented at the 7th International Laser Radar Conference at SRI Menlo Park, CA, November 1975.
7. Van de Hulst, H. C., 1957, Light Scattering by Small Particles, John Wiley and Sons, Inc., New York.

DISTRIBUTION LIST

Dr. Frank D. Eaton
Geophysical Institute
University of Alaska
Fairbanks, AK 99701

Commander
US Army Aviation Center
ATTN: ATZQ-D-MA
Fort Rucker, AL 36362

Chief, Atmospheric Sciences Div
Code ES-81
NASA
Marshall Space Flight Center,
AL 35812

Commander
US Army Missile R&D Command
ATTN: DRDMI-CGA (B. W. Fowler)
Redstone Arsenal, AL 35809

Redstone Scientific Information Center
ATTN: DRDMI-TBD
US Army Missile R&D Command
Redstone Arsenal, AL 35809

Commander
US Army Missile R&D Command
ATTN: DRDMI-TEM (R. Haraway)
Redstone Arsenal, AL 35809

Commander
US Army Missile R&D Command
ATTN: DRDMI-TRA (Dr. Essenwanger)
Redstone Arsenal, AL 35809

Commander
HQ, Fort Huachuca
ATTN: Tech Ref Div
Fort Huachuca, AZ 85613

Commander
US Army Intelligence Center & School
ATTN: ATSI-CD-MD
Fort Huachuca, AZ 85613

Commander
US Army Yuma Proving Ground
ATTN: Technical Library
Bldg 2100
Yuma, AZ 85364

Naval Weapons Center (Code 3173)
ATTN: Dr. A. Shlanta
China Lake, CA 93555

Sylvania Elec Sys Western Div
ATTN: Technical Reports Library
PO Box 205
Mountain View, CA 94040

Geophysics Officer
PMTC Code 3250
Pacific Missile Test Center
Point Mugu, CA 93042

Commander
Naval Ocean Systems Center (Code 4473)
ATTN: Technical Library
San Diego, CA 92152

Meteorologist in Charge
Kwajalein Missile Range
PO Box 67
APO San Francisco, 96555

Director
NOAA/ERL/APCL R31
RB3-Room 567
Boulder, CO 80302

Library-R-51-Tech Reports
NOAA/ERL
320 S. Broadway
Boulder, CO 80302

National Center for Atmos Research
NCAR Library
PO Box 3000
Boulder, CO 80307

R. B. Girardo
Bureau of Reclamation
E&R Center, Code 1220
Denver Federal Center, Bldg 67
Denver, CO 80225

National Weather Service
National Meteorological Center
W321, WWB, Room 201
ATTN: Mr. Quiroz
Washington, DC 20233

Mil Assistant for Atmos Sciences
Ofc of the Undersecretary of Defense
for Rsch & Engr/E&LS - Room 3D129
The Pentagon
Washington, DC 20301

Defense Communications Agency
Technical Library Center
Code 205
Washington, DC 20305

Director
Defense Nuclear Agency
ATTN: Technical Library
Washington, DC 20305

HQDA (DAEN-RDM/Dr. de Percin)
Washington, DC 20314

Director
Naval Research Laboratory
Code 5530
Washington, DC 20375

Commanding Officer
Naval Research Laboratory
Code 2627
Washington, DC 20375

Dr. J. M. MacCallum
Naval Research Laboratory
Code 1409
Washington, DC 20375

The Library of Congress
ATTN: Exchange & Gift Div
Washington, DC 20540
2

Head, Atmos Rsch Section
Div Atmospheric Science
National Science Foundation
1800 G. Street, NW
Washington, DC 20550

CPT Hugh Albers, Exec Sec
Interdept Committee on Atmos Science
National Science Foundation
Washington, DC 20550

Director, Systems R&D Service
Federal Aviation Administration
ATTN: ARD-54
2100 Second Street, SW
Washington, DC 20590

ADTC/DLODL
Eglin AFB, FL 32542

Naval Training Equipment Center
ATTN: Technical Library
Orlando, FL 32813

Det 11, 2WS/OI
ATTN: Maj Orondorff
Patrick AFB, FL 32925

USAFETAC/CB
Scott AFB, IL 62225

HQ, ESD/TOSI/S-22
Hanscom AFB, MA 01731

Air Force Geophysics Laboratory
ATTN: LCB (A. S. Carten, Jr.)
Hanscom AFB, MA 01731

Air Force Geophysics Laboratory
ATTN: LYD
Hanscom AFB, MA 01731

Meteorology Division
AFGL/LY
Hanscom AFB, MA 01731

US Army Liaison Office
MIT-Lincoln Lab, Library A-082
PO Box 73
Lexington, MA 02173

Director
US Army Ballistic Rsch Lab
ATTN: DRDAR-BLB (Dr. G. E. Keller)
Aberdeen Proving Ground, MD 21005

Commander
US Army Ballistic Rsch Lab
ATTN: DRDAR-BLP
Aberdeen Proving Ground, MD 21005

Director
US Army Armament R&D Command
Chemical Systems Laboratory
ATTN: DRDAR-CLJ-I
Aberdeen Proving Ground, MD 21010

Chief CB Detection & Alarms Div
Chemical Systems Laboratory
ATTN: DRDAR-CLC-CR (H. Tannenbaum)
Aberdeen Proving Ground, MD 21010

Commander
Harry Diamond Laboratories
ATTN: DELHD-CO
2800 Powder Mill Road
Adelphi, MD 20783

Commander
ERADCOM
ATTN: DRDEL-AP
2800 Powder Mill Road
Adelphi, MD 20783
2

Commander
ERADCOM
ATTN: DRDEL-CG/DRDEL-DC/DRDEL-CS
2800 Powder Mill Road
Adelphi, MD 20783

Commander
ERADCOM
ATTN: DRDEL-CT
2800 Powder Mill Road
Adelphi, MD 20783

Commander
ERADCOM
ATTN: DRDEL-EA
2800 Powder Mill Road
Adelphi, MD 20783

Commander
ERADCOM
ATTN: DRDEL-PA/DRDEL-ILS/DRDEL-E
2800 Powder Mill Road
Adelphi, MD 20783

Commander
ERADCOM
ATTN: DRDEL-PAO (S. Kimmel)
2800 Powder Mill Road
Adelphi, MD 20783

Chief
Intelligence Materiel Dev & Support Ofc
ATTN: DELEW-WL-I
Bldg 4554
Fort George G. Meade, MD 20755

Acquisitions Section, IRDB-D823
Library & Info Service Div, NOAA
6009 Executive Blvd
Rockville, MD 20852

Naval Surface Weapons Center
White Oak Library
Silver Spring, MD 20910

The Environmental Research
Institute of MI
ATTN: IRIA Library
PO Box 8618
Ann Arbor, MI 48107

Mr. William A. Main
USDA Forest Service
1407 S. Harrison Road
East Lansing, MI 48823

Dr. A. D. Belmont
Research Division
PO Box 1249
Control Data Corp
Minneapolis, MN 55440

Director
Naval Oceanography & Meteorology
NSTL Station
Bay St Louis, MS 39529

Director
US Army Engr Waterways Experiment Sta
ATTN: Library
PO Box 631
Vicksburg, MS 39180

Environmental Protection Agency
Meteorology Laboratory
Research Triangle Park, NC 27711

US Army Research Office
ATTN: DRXRO-PP
PO Box 12211
Research Triangle Park, NC 27709

Commanding Officer
US Army Armament R&D Command
ATTN: DRDAR-TSS Bldg 59
Dover, NJ 07801

Commander
HQ, US Army Avionics R&D Activity
ATTN: DAVAA-O
Fort Monmouth, NJ 07703

Commander/Director
US Army Combat Surveillance & Target
Acquisition Laboratory
ATTN: DELCS-D
Fort Monmouth, NJ 07703

Commander
US Army Electronics R&D Command
ATTN: DELCS-S
Fort Monmouth, NJ 07703

US Army Materiel Systems
Analysis Activity
ATTN: DRXSY-MP
Aberdeen Proving Ground, MD 21005

Director
US Army Electronics Technology &
Devices Laboratory
ATTN: DELET-D
Fort Monmouth, NJ 07703

Commander
US Army Electronic Warfare Laboratory
ATTN: DELEW-D
Fort Monmouth, NJ 07703

Commander
US Army Night Vision &
Electro-Optics Laboratory
ATTN: DELNV-L (Dr. Rudolf Buser)
Fort Monmouth, NJ 07703

Commander
ERADCOM Technical Support Activity
ATTN: DELSD-L
Fort Monmouth, NJ 07703

Project Manager, FIREFINDER
ATTN: DRCPM-FF
Fort Monmouth, NJ 07703

Project Manager, REMBASS
ATTN: DRCPM-RBS
Fort Monmouth, NJ 07703

Commander
US Army Satellite Comm Agency
ATTN: DRCPM-SC-3
Fort Monmouth, NJ 07703

Commander
ERADCOM Scientific Advisor
ATTN: DRDEL-SA
Fort Monmouth, NJ 07703

6585 TG/WE
Holloman AFB, NM 88330

AFWL/WE
Kirtland, AFB, NM 87117

AFWL/Technical Library (SUL)
Kirtland AFB, NM 87117

Commander
US Army Test & Evaluation Command
ATTN: STEWS-AD-L
White Sands Missile Range, NM 88002

Rome Air Development Center
ATTN: Documents Library
TSLD (Bette Smith)
Griffiss AFB, NY 13441

Commander
US Army Tropic Test Center
ATTN: STETC-TD (Info Center)
APO New York 09827

Commandant
US Army Field Artillery School
ATTN: ATSF-CD-R (Mr. Farmer)
Fort Sill, OK 73503

Commandant
US Army Field Artillery School
ATTN: ATSF-CF-R
Fort Sill, OK 73503

Director CFD
US Army Field Artillery School
ATTN: Met Division
Fort Sill, OK 73503

Commandant
US Army Field Artillery School
ATTN: Morris Swett Library
Fort Sill, OK 73503

Commander
US Army Dugway Proving Ground
ATTN: MT-DA-L
Dugway, UT 84022

Dr. C. R. Sreedrahan
Research Associates
Utah State University, UNC 48
Logan, UT 84322

Inge Dirmhirn, Professor
Utah State University, UNC 48
Logan, UT 84322

Defense Documentation Center
ATTN: DDC-TCA
Cameron Station Bldg 5
Alexandria, VA 22314
12

Commanding Officer
US Army Foreign Sci & Tech Center
ATTN: DRXST-IS1
220 7th Street, NE
Charlottesville, VA 22901

Naval Surface Weapons Center
Code G65
Dahlgren, VA 22448

Commander
US Army Night Vision
& Electro-Optics Lab
ATTN: DELNV-D
Fort Belvoir, VA 22060

Commander and Director
US Army Engineer Topographic Lab
ETL-TD-MB
Fort Belvoir, VA 22060

Director
Applied Technology Lab
DAVDL-EU-TSD
ATTN: Technical Library
Fort Eustis, VA 23604

Department of the Air Force
OL-C, 5WW
Fort Monroe, VA 23651

Department of the Air Force
5WW/DN
Langley AFB, VA 23665

Director
Development Center MCDEC
ATTN: Firepower Division
Quantico, VA 22134

US Army Nuclear & Chemical Agency
ATTN: MONA-WE
Springfield, VA 22150

Director
US Army Signals Warfare Laboratory
ATTN: DELSW-OS (Dr. R. Burkhardt)
Vint Hill Farms Station
Warrenton, VA 22186

Commander
US Army Cold Regions Test Center
ATTN: STECR-OP-PM
APO Seattle, WA 98733

Dr. John L. Walsh
Code 5560
Navy Research Lab
Washington, DC 20375

Commander
TRASANA
ATTN: ATAA-PL
(Dolores Anguiano)
White Sands Missile Range, NM 88002

Commander
US Army Dugway Proving Ground
ATTN: STEDP-MT-DA-M (Mr. Paul Carlson)
Dugway, UT 84022

Commander
US Army Dugway Proving Ground
ATTN: STEDP-MT-DA-T
(Mr. William Peterson)
Dugway, UT 84022

Commander
USATRADO
ATTN: ATCD-SIE
Fort Monroe, VA 23651

Commander
USATRADO
ATTN: ATCD-CF
Fort Monroe, VA 23651

Commander
USATRADO
ATTN: Tech Library
Fort Monroe, VA 23651

ATMOSPHERIC SCIENCES RESEARCH PAPERS

1. Lindberg, J.D., "An Improvement to a Method for Measuring the Absorption Coefficient of Atmospheric Dust and other Strongly Absorbing Powders," ECOM-5565, July 1975.
2. Avara, Elton P., "Mesoscale Wind Shears Derived from Thermal Winds," ECOM-5566, July 1975.
3. Gomez, Richard B., and Joseph H. Pierluissi, "Incomplete Gamma Function Approximation for King's Strong-Line Transmittance Model," ECOM-5567, July 1975.
4. Blanco, A.J., and B.F. Engebos, "Ballistic Wind Weighting Functions for Tank Projectiles," ECOM-5568, August 1975.
5. Taylor, Fredrick J., Jack Smith, and Thomas H. Pries, "Crosswind Measurements through Pattern Recognition Techniques," ECOM-5569, July 1975.
6. Walters, D.L., "Crosswind Weighting Functions for Direct-Fire Projectiles," ECOM-5570, August 1975.
7. Duncan, Louis D., "An Improved Algorithm for the Iterated Minimal Information Solution for Remote Sounding of Temperature," ECOM-5571, August 1975.
8. Robbiani, Raymond L., "Tactical Field Demonstration of Mobile Weather Radar Set AN/TPS-41 at Fort Rucker, Alabama," ECOM-5572, August 1975.
9. Miers, B., G. Blackman, D. Langer, and N. Lorimier, "Analysis of SMS/GOES Film Data," ECOM-5573, September 1975.
10. Manquero, Carlos, Louis Duncan, and Rufus Bruce, "An Indication from Satellite Measurements of Atmospheric CO₂ Variability," ECOM-5574, September 1975.
11. Petracca, Carmine, and James D. Lindberg, "Installation and Operation of an Atmospheric Particulate Collector," ECOM-5575, September 1975.
12. Avara, Elton P., and George Alexander, "Empirical Investigation of Three Iterative Methods for Inverting the Radiative Transfer Equation," ECOM-5576, October 1975.
13. Alexander, George D., "A Digital Data Acquisition Interface for the SMS Direct Readout Ground Station - Concept and Preliminary Design," ECOM-5577, October 1975.
14. Cantor, Israel, "Enhancement of Point Source Thermal Radiation Under Clouds in a Nonattenuating Medium," ECOM-5578, October 1975.
15. Norton, Colburn, and Glenn Hoidale, "The Diurnal Variation of Mixing Height by Month over White Sands Missile Range, N.M.," ECOM-5579, November 1975.
16. Avara, Elton P., "On the Spectrum Analysis of Binary Data," ECOM-5580, November 1975.
17. Taylor, Fredrick J., Thomas H. Pries, and Chao-Huan Huang, "Optimal Wind Velocity Estimation," ECOM-5581, December 1975.
18. Avara, Elton P., "Some Effects of Autocorrelated and Cross-Correlated Noise on the Analysis of Variance," ECOM-5582, December 1975.
19. Gillespie, Patti S., R.L. Armstrong, and Kenneth O. White, "The Spectral Characteristics and Atmospheric CO₂ Absorption of the Ho³⁺YLF Laser at 2.05 μ m," ECOM-5583, December 1975.
20. Novlan, David J. "An Empirical Method of Forecasting Thunderstorms for the White Sands Missile Range," ECOM-5584, February 1976.
21. Avara, Elton P., "Randomization Effects in Hypothesis Testing with Autocorrelated Noise," ECOM-5585, February 1976.
22. Watkins, Wendell R., "Improvements in Long Path Absorption Cell Measurement," ECOM-5586, March 1976.
23. Thomas, Joe, George D. Alexander, and Marvin Dubbin, "SATTEL - An Army Dedicated Meteorological Telemetry System," ECOM-5587, March 1976.
24. Kennedy, Bruce W., and Delbert Bynum, "Army User Test Program for the RDT&E-XM-75 Meteorological Rocket," ECOM-5588, April 1976.

25. Barnett, Kenneth M., "A Description of the Artillery Meteorological Comparisons at White Sands Missile Range, October 1974 - December 1974 ('PASS' - Prototype Artillery [Meteorological] Subsystem)," ECOM-5589, April 1976.
26. Miller, Walter B., "Preliminary Analysis of Fall-of-Shot From Project 'PASS'," ECOM-5590, April 1976.
27. Avara, Elton P., "Error Analysis of Minimum Information and Smith's Direct Methods for Inverting the Radiative Transfer Equation," ECOM-5591, April 1976.
28. Yee, Young P., James D. Horn, and George Alexander, "Synoptic Thermal Wind Calculations from Radiosonde Observations Over the Southwestern United States," ECOM-5592, May 1976.
29. Duncan, Louis D., and Mary Ann Seagraves, "Applications of Empirical Corrections to NOAA-4 VTPR Observations," ECOM-5593, May 1976.
30. Miers, Bruce T., and Steve Weaver, "Applications of Meteorological Satellite Data to Weather Sensitive Army Operations," ECOM-5594, May 1976.
31. Sharenow, Moses, "Redesign and Improvement of Balloon ML-566," ECOM-5595, June, 1976.
32. Hansen, Frank V., "The Depth of the Surface Boundary Layer," ECOM-5596, June 1976.
33. Pinnick, R.G., and E.B. Stenmark, "Response Calculations for a Commercial Light-Scattering Aerosol Counter," ECOM-5597, July 1976.
34. Mason, J., and G.B. Hoidale, "Visibility as an Estimator of Infrared Transmittance," ECOM-5598, July 1976.
35. Bruce, Rufus E., Louis D. Duncan, and Joseph H. Pierluissi, "Experimental Study of the Relationship Between Radiosonde Temperatures and Radiometric-Area Temperatures," ECOM-5599, August 1976.
36. Duncan, Louis D., "Stratospheric Wind Shear Computed from Satellite Thermal Sounder Measurements," ECOM-5800, September 1976.
37. Taylor, F., P. Mohan, P. Joseph and T. Pries, "An All Digital Automated Wind Measurement System," ECOM-5801, September 1976.
38. Bruce, Charles, "Development of Spectrophones for CW and Pulsed Radiation Sources," ECOM-5802, September 1976.
39. Duncan, Louis D., and Mary Ann Seagraves, "Another Method for Estimating Clear Column Radiances," ECOM-5803, October 1976.
40. Blanco, Abel J., and Larry E. Taylor, "Artillery Meteorological Analysis of Project Pass," ECOM-5804, October 1976.
41. Miller, Walter, and Bernard Engebos, "A Mathematical Structure for Refinement of Sound Ranging Estimates," ECOM-5805, November, 1976.
42. Gillespie, James B., and James D. Lindberg, "A Method to Obtain Diffuse Reflectance Measurements from 1.0 to 3.0 μm Using a Cary 17I Spectrophotometer," ECOM-5806, November 1976.
43. Rubio, Roberto, and Robert O. Olsen, "A Study of the Effects of Temperature Variations on Radio Wave Absorption," ECOM-5807, November 1976.
44. Ballard, Harold N., "Temperature Measurements in the Stratosphere from Balloon-Borne Instrument Platforms, 1968-1975," ECOM-5808, December 1976.
45. Monahan, H.H., "An Approach to the Short-Range Prediction of Early Morning Radiation Fog," ECOM-5809, January 1977.
46. Engebos, Bernard Francis, "Introduction to Multiple State Multiple Action Decision Theory and Its Relation to Mixing Structures," ECOM-5810, January 1977.
47. Low, Richard D.H., "Effects of Cloud Particles on Remote Sensing from Space in the 10-Micrometer Infrared Region," ECOM-5811, January 1977.
48. Bonner, Robert S., and R. Newton, "Application of the AN/GVS-5 Laser Rangefinder to Cloud Base Height Measurements," ECOM-5812, February 1977.
49. Rubio, Roberto, "Lidar Detection of Subvisible Reentry Vehicle Erosive Atmospheric Material," ECOM-5813, March 1977.
50. Low, Richard D.H., and J.D. Horn, "Mesoscale Determination of Cloud-Top Height: Problems and Solutions," ECOM-5814, March 1977.

51. Duncan, Louis D., and Mary Ann Seagraves, "Evaluation of the NOAA-4 VTPR Thermal Winds for Nuclear Fallout Predictions," ECOM-5815, March 1977.
52. Randhawa, Jagir S., M. Izquierdo, Carlos McDonald and Zvi Salpeter, "Stratospheric Ozone Density as Measured by a Chemiluminescent Sensor During the Stratcom VI-A Flight," ECOM-5816, April 1977.
53. Rubio, Roberto, and Mike Izquierdo, "Measurements of Net Atmospheric Irradiance in the 0.7- to 2.8-Micrometer Infrared Region," ECOM-5817, May 1977.
54. Ballard, Harold N., Jose M. Serna, and Frank P. Hudson Consultant for Chemical Kinetics, "Calculation of Selected Atmospheric Composition Parameters for the Mid-Latitude, September Stratosphere," ECOM-5818, May 1977.
55. Mitchell, J.D., R.S. Sagar, and R.O. Olsen, "Positive Ions in the Middle Atmosphere During Sunrise Conditions," ECOM-5819, May 1977.
56. White, Kenneth O., Wendell R. Watkins, Stuart A. Schleusener, and Ronald L. Johnson, "Solid-State Laser Wavelength Identification Using a Reference Absorber," ECOM-5820, June 1977.
57. Watkins, Wendell R., and Richard G. Dixon, "Automation of Long-Path Absorption Cell Measurements," ECOM-5821, June 1977.
58. Taylor, S.E., J.M. Davis, and J.B. Mason, "Analysis of Observed Soil Skin Moisture Effects on Reflectance," ECOM-5822, June 1977.
59. Duncan, Louis D. and Mary Ann Seagraves, "Fallout Predictions Computed from Satellite Derived Winds," ECOM-5823, June 1977.
60. Snider, D.E., D.G. Murcay, F.H. Murcay, and W.J. Williams, "Investigation of High-Altitude Enhanced Infrared Background Emissions" (U), SECRET, ECOM-5824, June 1977.
61. Dubbin, Marvin H. and Dennis Hall, "Synchronous Meteorological Satellite Direct Readout Ground System Digital Video Electronics," ECOM-5825, June 1977.
62. Miller, W., and B. Engebos, "A Preliminary Analysis of Two Sound Ranging Algorithms," ECOM-5826, July 1977.
63. Kennedy, Bruce W., and James K. Luers, "Ballistic Sphere Techniques for Measuring Atmospheric Parameters," ECOM-5827, July 1977.
64. Duncan, Louis D., "Zenith Angle Variation of Satellite Thermal Sounder Measurements," ECOM-5828, August 1977.
65. Hansen, Frank V., "The Critical Richardson Number," ECOM-5829, September 1977.
66. Ballard, Harold N., and Frank P. Hudson (Compilers), "Stratospheric Composition Balloon-Borne Experiment," ECOM-5830, October 1977.
67. Barr, William C., and Arnold C. Peterson, "Wind Measuring Accuracy Test of Meteorological Systems," ECOM-5831, November 1977.
68. Ethridge, G.A. and F.V. Hansen, "Atmospheric Diffusion: Similarity Theory and Empirical Derivations for Use in Boundary Layer Diffusion Problems," ECOM-5832, November 1977.
69. Low, Richard D.H., "The Internal Cloud Radiation Field and a Technique for Determining Cloud Blackness," ECOM-5833, December 1977.
70. Watkins, Wendell R., Kenneth O. White, Charles W. Bruce, Donald L. Walters, and James D. Lindberg, "Measurements Required for Prediction of High Energy Laser Transmission," ECOM-5834, December 1977.
71. Rubio, Robert, "Investigation of Abrupt Decreases in Atmospherically Backscattered Laser Energy," ECOM-5835, December 1977.
72. Monahan, H.H. and R.M. Cionco, "An Interpretative Review of Existing Capabilities for Measuring and Forecasting Selected Weather Variables (Emphasizing Remote Means)," ASL-TR-0001, January 1978.
73. Heaps, Melvin G., "The 1979 Solar Eclipse and Validation of D-Region Models," ASL-TR-0002, March 1978.

74. Jennings, S.G., and J.B. Gillespie, "M.I.E. Theory Sensitivity Studies - The Effects of Aerosol Complex Refractive Index and Size Distribution Variations on Extinction and Absorption Coefficients Part II: Analysis of the Computational Results," ASL-TR-0003, March 1978.
75. White, Kenneth O. et al, "Water Vapor Continuum Absorption in the 3.5 μ m to 4.0 μ m Region," ASL-TR-0004, March 1978.
76. Olsen, Robert O., and Bruce W. Kennedy, "ABRES Pretest Atmospheric Measurements," ASL-TR-0005, April 1978.
77. Ballard, Harold N., Jose M. Serna, and Frank P. Hudson, "Calculation of Atmospheric Composition in the High Latitude September Stratosphere," ASL-TR-0006, May 1978.
78. Watkins, Wendell R. et al, "Water Vapor Absorption Coefficients at HF Laser Wavelengths," ASL-TR-0007, May 1978.
79. Hansen, Frank V., "The Growth and Prediction of Nocturnal Inversions," ASL-TR-0008, May 1978.
80. Samuel, Christine, Charles Bruce, and Ralph Brewer, "Spectrophone Analysis of Gas Samples Obtained at Field Site," ASL-TR-0009, June 1978.
81. Pinnick, R.G. et al., "Vertical Structure in Atmospheric Fog and Haze and its Effects on IR Extinction," ASL-TR-0010, July 1978.
82. Low, Richard D.H., Louis D. Duncan, and Richard B. Gomez, "The Microphysical Basis of Fog Optical Characterization," ASL-TR-0011, August 1978.
83. Heaps, Melvin G., "The Effect of a Solar Proton Event on the Minor Neutral Constituents of the Summer Polar Mesosphere," ASL-TR-0012, August 1978.
84. Mason, James B., "Light Attenuation in Falling Snow," ASL-TR-0013, August 1978.
85. Blanco, Abel J., "Long-Range Artillery Sound Ranging: "PASS" Meteorological Application," ASL-TR-0014, September 1978.
86. Heaps, M.G., and F.F. Niles, "Modeling the Ion Chemistry of the D-Region: A case Study Based Upon the 1966 Total Solar Eclipse," ASL-TR-0015, September 1978.
87. Jennings, S.G., and R.G. Pinnick, "Effects of Particulate Complex Refractive Index and Particle Size Distribution Variations on Atmospheric Extinction and Absorption for Visible Through Middle-Infrared Wavelengths," ASL-TR-0016, September 1978.
88. Watkins, Wendell R., Kenneth O. White, Lanny R. Bower, and Brian Z. Sojka, "Pressure Dependence of the Water Vapor Continuum Absorption in the 3.5- to 4.0-Micrometer Region," ASL-TR-0017, September 1978.
89. Miller, W.B., and B.F. Engebos, "Behavior of Four Sound Ranging Techniques in an Idealized Physical Environment," ASL-TR-0018, September 1978.
90. Gomez, Richard G., "Effectiveness Studies of the CBU-88/B Bomb, Cluster, Smoke Weapon" (U), CONFIDENTIAL ASL-TR-0019, September 1978.
91. Miller, August, Richard C. Shirkey, and Mary Ann Seagraves, "Calculation of Thermal Emission from Aerosols Using the Doubling Technique," ASL-TR-0020, November, 1978.
92. Lindberg, James D. et al., "Measured Effects of Battlefield Dust and Smoke on Visible, Infrared, and Millimeter Wavelengths Propagation: A Preliminary Report on Dusty Infrared Test-1 (DIRT-1)," ASL-TR-0021, January 1979.
93. Kennedy, Bruce W., Arthur Kinghorn, and B.R. Hixon, "Engineering Flight Tests of Range Meteorological Sounding System Radiosonde," ASL-TR-0022, February 1979.
94. Rubio, Roberto, and Don Hoock, "Microwave Effective Earth Radius Factor Variability at Wiesbaden and Balboa," ASL-TR-0023, February 1979.
95. Low, Richard D.H., "A Theoretical Investigation of Cloud/Fog Optical Properties and Their Spectral Correlations," ASL-TR-0024, February 1979.

96. Pinnick, R.G., and H. J. Auvermann, "Response Characteristics of Knollenberg Light-Scattering Aerosol Counters," ASL-TR-0025, February 1979.
97. Heaps, Melvin G., Robert O. Olsen, and Warren W. Berning, "Solar Eclipse 1979, Atmospheric Sciences Laboratory Program Overview," ASL-TR-0026 February 1979.
98. Blanco, Abel J., "Long-Range Artillery Sound Ranging: 'PASS' GR-8 Sound Ranging Data," ASL-TR-0027, March 1979.
99. Kennedy, Bruce W., and Jose M. Serna, "Meteorological Rocket Network System Reliability," ASL-TR-0028, March 1979.
100. Swingle, Donald M., "Effects of Arrival Time Errors in Weighted Range Equation Solutions for Linear Base Sound Ranging," ASL-TR-0029, April 1979.
101. Umstead, Robert K., Ricardo Pena, and Frank V. Hansen, "KWIK: An Algorithm for Calculating Munition Expenditures for Smoke Screening/Obscuration in Tactical Situations," ASL-TR-0030, April 1979
102. D'Arcy, Edward M., "Accuracy Validation of the Modified Nike Hercules Radar," ASL-TR-0031, May, 1979
103. Rodriguez, Ruben, "Evaluation of the Passive Remote Crosswind Sensor," ASL-TR-0032, May 1979
104. Barber, T.L., and R. Rodriguez, "Transit Time Lidar Measurement of Near-Surface Winds in the Atmosphere," ASL-TR-0033, May 1979